

1 Light Absorption Enhancement of Black Carbon in Urban Beijing in
2 Summer

3
4 Conghui Xie^{1,2}, Weiqi Xu^{1,2}, Junfeng Wang^{3,a}, Dantong Liu⁴, Xinlei Ge³, Qi Zhang⁵, Qingqing
5 Wang¹, Wei Du^{1,2,b}, Jian Zhao^{1,2}, Wei Zhou^{1,2}, Jie Li¹, Pingqing Fu^{6,2}, Zifa Wang^{1,2,8}, Douglas
6 Worsnop⁷, Yele Sun^{1,2,8*}

7
8 ¹State Key Laboratory of Atmospheric Boundary Layer Physics and Atmospheric Chemistry,
9 Institute of Atmospheric Physics, Chinese Academy of Sciences, Beijing 100029, China

10 ²College of Earth and Planetary Sciences, University of Chinese Academy of Sciences, Beijing
11 100049, China

12 ³School of Environmental Science and Engineering, Nanjing University of Information Science &
13 Technology, Nanjing 210044, China

14 ⁴Department of Atmospheric Sciences, School of Earth Sciences, Zhejiang University, Hangzhou,
15 Zhejiang, China

16 ⁵Department of Environmental Toxicology, University of California, 1 Shields Ave., Davis, CA
17 95616, USA

18 ⁶Institute of Surface-Earth System Science, Tianjin University, Tianjin 300072, China

19 ⁷Aerodyne Research, Inc., Billerica, MA 01821, USA

20 ⁸Center for Excellence in Regional Atmospheric Environment, Institute of Urban Environment,
21 Chinese Academy of Sciences, Xiamen 361021, China

22 ^anow at: School of Engineering and Applied Sciences, Harvard University, Cambridge 02138, USA

23 ^bnow at: Institute for Atmospheric and Earth System Research / Physics, Faculty of Science,
24 University of Helsinki, Helsinki, Finland

25

26 Correspondence: Yele Sun (sunyele@mail.iap.ac.cn)

27 **ABSTRACT**

28 The light absorption enhancement (E_{abs}) of black carbon (BC) caused by non-BC materials is an
29 important source of uncertainty in radiative forcing estimate, yet remains poorly understood in
30 relatively polluted environment such as the megacity Beijing. Here BC absorption enhancement at
31 630 nm was *in-situ* measured using a thermodenuder coupled with a soot particle aerosol mass
32 spectrometer and a single scattering albedo monitor in Beijing in summer. The project average ($\pm 1\sigma$)
33 E_{abs} was 1.59 (± 0.26), suggesting a significant amplification of BC absorption due to coating
34 materials. E_{abs} presented a clear daytime increase due to enhanced photochemical processing, and a
35 strong dependence on the mass ratios of non-BC coatings to BC (R_{BC}). Our results showed that the
36 increase in E_{abs} as a function of R_{BC} was mainly caused by the increased contributions of secondary
37 aerosol. Further analysis showed that the BC absorption enhancement in summer in Beijing was
38 mainly associated with secondary formation of nitrate, sulfate and highly oxidized secondary organic
39 aerosol (SOA), while the formation of freshly and less oxidized SOA appeared not to play an
40 important role.

41

42 **Key Words:**

43 Black carbon; Absorption enhancement; Secondary aerosol; Beijing

44 **1 Introduction**

45 Black carbon aerosol (BC), a by-product of incomplete combustion carbonaceous matter (e.g.
46 biomass and fossil fuel) is recognized as the third most important global warming agent after CO₂
47 and CH₄ (Stocker et al., 2013). BC exerts a great impact on climate change by absorbing direct solar
48 radiation, reducing cloud albedo, and accelerating the melt of snow (Bond et al., 2013). Accurate
49 estimate of light absorption of BC is thus important to improve our understanding on the impacts of
50 these processes on climate radiative forcing.

51 The BC absorption is enhanced by its coating materials (Lack and Cappa, 2010), and the
52 enhancement can be significant by a factor of ~2 when BC is internally mixed with other
53 components (Bond and Bergstrom, 2006; Chandra, 2004; Shiraiwa et al., 2010). In contrast, the
54 freshly emitted BC tend to be fractal-like and externally mixed with other components (Peng et al.,
55 2016), and has no absorption enhancement (Liu et al., 2017). The freshly emitted BC can be aged
56 rapidly in the atmosphere (Glen, 2010; Moteki et al., 2007), which changes the mixing state,
57 morphology, coating thickness of BC and thereby its absorbing properties. Current climate models
58 usually use a constant enhancement factor (~1.5) to estimate the radiative forcing of BC (Chung and
59 Seinfeld, 2008; Wang et al., 2014b). However, a recent study showed that the BC absorption
60 enhancements (E_{abs}) should be treated as a function of particle mixing state (Liu et al., 2017).
61 Previous studies also showed significant differences in BC absorption enhancement in different
62 regions. For example, the field measurements during CALNex and CARES in California showed
63 small BC enhancements (~ 6%) and the enhancements were weakly dependent on photochemical
64 aging (Cappa et al., 2012). Small absorption enhancement were also observed at Nagoya (Japan)

65 (Nakayama et al., 2015) and Shenzhen in China(Lan et al., 2013), due to the fact that a large fraction
66 of aerosol species was externally mixed with BC. Liu et al (2015) found that the magnitude of BC
67 absorption enhancement depends strongly on coating amount, which varies largely for different
68 sources and regions. In fact, light absorption enhancement of $\sim 1.8 - 2.2$ were observed in heavily
69 polluted areas such as Indo-Gangetic Plain (Thamban et al., 2017), Xi'an (Wang et al., 2014a), and
70 Yucheng(Cui et al., 2016). Peng et al. (2016) found that BC in polluted urban environment (Beijing,
71 China) aged much faster than that in a relatively clean area (Houston, USA), and the absorption
72 enhancement can be up to a factor of 2.4 in a few hours' ageing. Despite previous efforts in
73 characterization of BC absorption enhancements in different regions, *in situ* measurements of E_{abs} is
74 still limited, particularly in relatively polluted region in China.

75 In this work, the E_{abs} of BC was measured in urban Beijing in summer using a thermodenuder
76 coupled with a soot particle aerosol mass spectrometer (SP-AMS) and a cavity attenuated phase shift
77 single scattering albedo monitor (CAPS PM_{ssa}). The variation of E_{abs} in Beijing in summer and its
78 relationship with BC coating materials are elucidated, and the major factors affecting E_{abs} are
79 investigated.

80 **2 Experimental methods**

81 All measurements were conducted from 4 June to 13 June, 2017 at the Institute of Atmospheric
82 Physics (IAP), Chinese Academy of Sciences (39°58'28"N, 116°22'16"E) (Sun et al., 2012), which is
83 located between north 3rd and 4th ring roads in Beijing. The instruments were deployed on the roof of
84 a two-story building (~ 8 m). Ambient air was first drawn into the sampling room through a 1/2 inch

85 stainless steel tubing with a flow rate of 3 L min^{-1} . After passing through a diffusion silica-gel dryer,
86 aerosol particles ($\sim 1.5 \text{ L min}^{-1}$) were sub-sampled into a thermodenuder (TD), and then measured by
87 a SP-AMS and a CAPS PM_{ssa} . The SP-AMS removed the tungsten vaporizer and measured
88 refractory BC (rBC) and rBC-containing species only. The CAPS PM_{ssa} measured particle extinction
89 (b_{ext}) and scattering coefficients (b_{sca}) at 630 nm, and the difference between b_{ext} and b_{sca} was
90 absorption coefficient (b_{abs}). Although the b_{sca} measurements had uncertainties due to truncation
91 effects, our previous studies showed that such an effect was small, and b_{abs} derived from the CAPS
92 PM_{ssa} was highly correlated with that measured by photoacoustic extinctions and aethalometer
93 (Han et al., 2015; Xie et al., 2019). In this study, the measurements were alternated between TD and
94 bypass line every 10 min (Fig. S1), and the TD cycled through four temperature gradients (50, 100,
95 150, and 260 °C). The TD loss was corrected with rBC measured by the SP-AMS considering that
96 rBC does not evaporate at 260 °C. The meteorological data including temperature, relative humidity,
97 wind speed and wind direction (Fig. S2) were obtained from the measurements on the Beijing 325 m
98 meteorological tower.

99 In addition, a single-particle soot photometer (SP2, Droplet Measurement Technologies) was
100 used to measure the spherical equivalent core diameter (D_c) and the particle diameter (D_p) at the
101 same site (Liu et al., 2018). The D_p/D_c in this study is calculated as the bulk relative coating
102 thickness which reflects the integrated coated BC volume and uncoated BC core volume for a given
103 time window. The bulk D_p/D_c is largely independent of the uncertainties arising from smaller
104 particles because of their less important contribution to the integrated volume, therefore, the retrieval
105 rate of successful coating thickness decreases at smaller and larger D_c , because of the reduced

106 signal-to-noise level for the scattering signal of smaller particle and the detector saturation for larger
107 particle. The uncertainty associated with the missing single particle coating information is examined
108 at each D_c range by extrapolating the coating thickness at the most populated BC in mass with
109 coating retrieval rate $> 80\%$. The resulting uncertainties are by 7-11% for the BC with bulk $D_p/D_c > 2$,
110 3-8% at D_p/D_c 1.5-2 and 0.5-3% with D_p/D_c 1-1.5. Recent study indicates this bulk D_p/D_c metric is
111 able to produce the total coating mass associated with BC particles within 25% (Ting et al., 2018).

112 The E_{abs} was calculated as the ratio of ambient particle absorption ($b_{\text{abs, ambient}}$) to that passing
113 through the TD at 260 °C ($b_{\text{abs, TD}}$). As shown in Fig. S3, 76% of non-BC aerosol species evaporated
114 at 260 °C, and the remaining fraction was dominated by rBC and hydrocarbon-like OA(HOA)-rich
115 primary aerosol and more oxidized oxygenated OA (MO-OOA) that were resolved from positive
116 matrix factorization of high-resolution mass spectra of OA of the SP-AMS (Wang et al., 2019b).
117 Therefore, E_{abs} might have a slight underestimation due to the lensing effect of residual materials on
118 BC. $E_{\text{abs, MAC}}$ can also be estimated as the ratio of measured mass absorption coefficient ($\text{MAC}_{\text{obs}} =$
119 $b_{\text{abs, ambient}}/r\text{BC}$) to the reference MAC ($\text{MAC}_{\text{ref}} = 6.55 \text{ m}^2 \text{ g}^{-1}$) for uncoated BC at 630 nm. The
120 MAC_{ref} was derived from the power law dependence of absorption on wavelength with a MAC of
121 $7.5 \text{ m}^2 \text{ g}^{-1}$ at 550 nm (Bond and Bergstrom, 2006). E_{abs} was well correlated with $E_{\text{abs, MAC}}$ ($r^2 = 0.66$),
122 and the average values were also close (1.59 ± 0.26 and 1.63 ± 0.41 , respectively), suggesting that
123 these two methods were overall consistent. Therefore, E_{abs} discussed below referred to the TD-CAPS
124 method unless otherwise stated.

125 **3 Results and discussion**

126 The average ($\pm 1\sigma$) E_{abs} was 1.59 (± 0.26) for the entire study suggesting approximately 60%
127 light absorption enhancement by BC coatings. Such an enhancement was overall consistent with
128 ~ 1.5 that is often used in current climate models (Flanner et al., 2007), and agreed with the recent
129 observations at the SIRTA facility (Zhang et al., 2018a) and UK winter (Liu et al., 2015). However, it
130 was much higher than that previously reported in California regions with limited BC absorption
131 enhancement due to coatings (Cappa et al., 2019).

132 E_{abs} depends strongly on the mass ratios of coating materials on BC to rBC (R_{BC}) that were from
133 the SP-AMS measurements in Beijing in summer. As shown in Fig. 1a, E_{abs} increased substantially as
134 a function of R_{BC} . As R_{BC} increased from 2 to 6, E_{abs} increased by 45% from 1.34 to 1.94. Such an
135 R_{BC} dependence of E_{abs} was remarkably similar to that observed in UK winter although aerosol
136 composition was substantially different (Liu et al., 2015). However, we did not observe further
137 increases in E_{abs} as R_{BC} was larger than 6. One explanation was the few data points increasing the
138 uncertainties for E_{abs} estimates. Another possibility is that E_{abs} was stabilized as BC was fully aged
139 with a high R_{BC} (Wu et al., 2018). Fig. 1b shows that the aerosol composition of rBC coatings varied
140 significantly as a function of R_{BC} . As R_{BC} increased from 2 to 6, the mass fraction of non-BC POA
141 (rBC-rich+HOA-rich) decreased from 54% to 14%, while the contributions of secondary aerosol
142 species (= SOA+SIA) increased from 45% to 85%. These results indicate that the increases in E_{abs} of
143 BC were mainly caused by the enhanced contributions from secondary formation in Beijing in
144 summer. Comparatively, the fractions of primary and secondary aerosol species were relatively stable
145 during periods with $R_{\text{BC}} > 6$, which might also explain the negligible increases of E_{abs} . Compared

146 with summer, our previous winter studies in 2016 showed that non-BC aerosol composition was
 147 dominated by POA (> ~60%) at $R_{BC} < 4.5$, and the contribution of secondary aerosol species
 148 increased rapidly to ~80% as R_{BC} increased up to 7. As a result, the MAC of BC at 630 nm in winter
 149 was relatively stable below $R_{BC} < 4.5$, and then increased by approximately 40% during periods with
 150 high R_{BC} (Xie et al., 2019). This is consistent with the conclusion in summer that BC absorption
 151 enhancement was mainly associated with secondary coatings, while the influences of non-BC POA
 152 on E_{abs} were generally small.

153 We also compared the measured E_{abs} with that derived from the Mie core-shell model by
 154 assuming refractive index of rBC core and coatings at 550 nm as $1.95+0.79i$ and $1.50+0i$,
 155 respectively (Liu et al., 2018). The R_{BC} from SP2 measurements was calculated using Eq. 1. The
 156 density of rBC is 1.8 g cm^{-3} and that ($1.3 \pm 0.05 \text{ g cm}^{-3}$) of coatings was estimated based on the
 157 chemical composition of BC-containing aerosol particles (Zhao et al., 2017).

$$158 \quad R_{BC} = \left(\left(\frac{D_p}{D_c} \right)^3 - 1 \right) \times \frac{\rho_{coating}}{\rho_{rBC}} \quad (1)$$

159 As shown in Fig. 1a, the R_{BC} dependence of simulated E_{abs} was similar, while the simulated E_{abs} were
 160 slightly lower than those from the ambient TD measurements (Fig. 1a).

161 Fig. 2a shows that E_{abs} increased as a function of particulate matter (PM) loadings suggesting
 162 stronger significant BC absorption enhancements during periods with higher pollution levels. For
 163 instance, E_{abs} increased from ~1.4 to 1.8 as PM_1 mass loading increased from ~10 to $50 \mu\text{g m}^{-3}$. We
 164 found that such enhancements were mainly associated with the increases in rBC coatings (R_{BC}),
 165 which is consistent with previously simulations (Zhang et al., 2018b) and chamber experiments in
 166 Beijing (Peng et al., 2016). However, we did not observe a clear rBC dependence of E_{abs} in summer,

167 consistent with the small variations in R_{BC} , and even slight decreases at high rBC loadings ($> 2 \mu\text{g}$
168 m^{-3}). This is different from winter when R_{BC} showed a considerable increase as a function of rBC
169 (Liu et al., 2018). Such differences can be explained by the differences in rBC sources and coating
170 materials between summer and winter. In winter, high rBC concentration was associated with high
171 POA from coal combustion and biomass burning emissions (Wang et al., 2019a), while in summer it
172 was dominantly from traffic emissions (Hu et al., 2016). The coating materials were also
173 substantially different between summer and winter. For example, SIA and SOA on average
174 accounted for 21% and 34% of the total BC-containing particle mass in summer (Xu et al., 2019),
175 while they were 20.1% and 20.8%, respectively in winter (Wang et al., 2019a). Previous studies
176 showed that rBC from traffic emissions has smaller R_{BC} compared with those from other combustion
177 sources, such as biomass burning and coal combustion (Liu et al., 2018). In fact, R_{BC} was
178 anticorrelated with rBC mass loading near vehicular emissions (Lee et al., 2017) while it was
179 positively correlated with rBC under high pollution with multiple sources of rBC (Lee et al., 2017;
180 Zhang et al., 2018b).

181 We further evaluated the influence of chemical composition of rBC coatings on E_{abs} . As shown
182 in Fig. 3, the changes in E_{abs} as a function of R_{BC} depended strongly on non-BC composition. The
183 periods with higher contributions of nitrate and sulfate showed correspondingly higher E_{abs}
184 throughout different R_{BC} . For example, E_{abs} was increased by 7 – 21% during periods with higher
185 nitrate contributions ($> 10\%$), while 6 – 17% for periods with higher sulfate contributions ($> 10\%$).
186 These results suggest that secondary nitrate and sulfate coated on BC have the most impacts on
187 absorption enhancement. One explanation is that the increased nitrate and sulfate changed the BC

188 mixing state to the core-shell structure and thus increased the absorption enhancement (He et al.,
189 2015). For example, recent studies showed that the increases in ammonium nitrate and sulfate can
190 reduce the deliquescence RH substantially and cause phase transitions of aerosol particles (Sun et al.,
191 2018). During periods with high contents of nitrate and sulfate, the BC-containing particles would be
192 more like in concentric core-shell structure due to the changes of particle phase states from solid to
193 aqueous phase, and hence lead to significant light absorption enhancement. Fig. 3 also shows very
194 different impacts of OA factors on BC absorption enhancement. The increased contribution of
195 MO-OOA presented a positive effect on absorption enhancement by approximately 6 – 7%. However,
196 LO-OOA and HOA decreased E_{abs} by 7 – 11% during periods with high contributions (10% and 15%,
197 respectively). Such results indicate that formation of freshly oxidized SOA in summer appears not an
198 important factor driving the increase of BC absorption enhancement. The decrease of E_{abs} as the
199 increase of HOA contribution was due to 1) vehicle emission with low R_{BC} has a very limited
200 influence on light absorption enhancement, and 2) the increase of HOA was associated with the
201 corresponding decreases in rBC coatings of sulfate, nitrate, and MO-OOA (Fig. 3). Considering that
202 E_{abs} calculated from the TD method could be affected by the residual mass at 260 °C, we further
203 checked the composition dependent relationship between $E_{\text{abs,MAC}}$ and R_{BC} (Fig. S4). As shown in
204 Fig. S4, similar conclusions were obtained that formation of secondary inorganic aerosol can impact
205 BC absorption enhancement significantly while that of SOA has limited influences and even
206 decreases E_{abs} . Our results were different from a recent study in the megacity of Paris, France
207 showing a major contributor of SOA to BC absorption enhancement in summer (Zhang et al., 2018a).
208 One reason was due to the very different aerosol composition between Beijing and Paris. While SOA

209 contributed more than half (52%) of submicron aerosol in Paris in summer, it was much lower (27%)
210 in Beijing.

211 The light absorption enhancement of BC presents a strong diurnal variation in Beijing in summer.
212 E_{abs} gradually increased from ~ 1.5 in the morning to ~ 1.8 at 12:00 – 13:00, and then decreased
213 slowly to 1.4 at midnight. Such a diurnal trend was overall similar to that of R_{BC} , photochemical age
214 indicated by $-\log(\text{NO}_x/\text{NO}_y)$, and ratios of secondary nitrate and sulfate to rBC (NO_3/rBC and
215 SO_4/rBC , respectively). These results indicate that photochemical processing played a dominant role
216 in changing rBC coatings and absorption enhancement in summer (Fig. 1c), which is different from
217 the observations in California (Cappa et al., 2012) showing limited dependence of E_{abs} on
218 photochemical aging. However, we also noticed the differences in aerosol composition and BC
219 mixing states before and after noontime. As shown in Fig. 4, NO_3/rBC showed the largest increase
220 from 8:00 to 12:00, while the variations in SO_4/rBC were relatively small, suggesting that the first
221 increase in E_{abs} in daytime was mainly driven by nitrate formation. Although SO_4/rBC ,
222 $\text{MO-OOA}/\text{rBC}$, and $-\log(\text{NO}_x/\text{NO}_y)$ continued to increase after noontime between 12:00 and 16:00,
223 E_{abs} decreased slowly instead. We found that R_{BC} and D_p/D_c remained relatively unchanged during
224 this period, while NO_3/rBC showed a clear decrease due to the evaporative loss of nitrate associated
225 with high temperature. Such results are consistent with the conclusion above that E_{abs} is sensitive to
226 the coating fractions of nitrate.

227 **4 Conclusion**

228 The absorption of BC remains a large uncertainty for estimating global warming due to the

229 controversial lensing effect of absorption enhancement. Here we provide direct evidence for BC
230 absorption enhancement in Beijing in summer using the *in situ* measurements by a thermodenuder
231 coupled with SP-AMS and single scattering albedo monitor. Our results showed that the average E_{abs}
232 at 630 nm was $1.59 (\pm 0.26)$ indicating a substantial absorption enhancement due to rBC coatings.
233 E_{abs} showed a strong dependence on rBC coatings (R_{BC}), and the increases in E_{abs} were mainly
234 caused by the production of secondary aerosol species. Further support was from the significant
235 daytime increase in E_{abs} that was associated with enhanced photochemical processing and the
236 formation of secondary organic and inorganic species. By characterizing the composition dependent
237 E_{abs} , we found that the increases in E_{abs} showed different sensitivities to different aerosol species.
238 Formation of secondary nitrate and sulfate in summer has the most impacts on BC absorption
239 enhancements, while freshly oxidized SOA appears not important. Our results highlight an urgent
240 need to characterize the changes of BC mixing states due to the formation of secondary organic and
241 inorganic aerosol species, and the changes of particle phase states.

242

243 **Acknowledgements.**

244 This work was supported by the National Natural Science Foundation of China (91744207,
245 41575120, 41571130034) and the National Key R&D Program of China (2017YFC0212704,
246 2017YFC0209601).

247 **Notes**

248 | The authors declare no competing financial interest.

249

250 **References**

- 251 Bond, T.C., Bergstrom, R.W., 2006. Light Absorption by Carbonaceous Particles: An Investigative
252 Review. *Aerosol Science and Technology* 40, 27-67.
- 253 Bond, T.C., Doherty, S.J., Fahey, D.W., Forster, P.M., Berntsen, T., DeAngelo, B.J., Flanner, M.G.,
254 Ghan, S., Kärcher, B., Koch, D., Kinne, S., Kondo, Y., Quinn, P.K., Sarofim, M.C., Schultz,
255 M.G., Schulz, M., Venkataraman, C., Zhang, H., Zhang, S., Bellouin, N., Guttikunda, S.K.,
256 Hopke, P.K., Jacobson, M.Z., Kaiser, J.W., Klimont, Z., Lohmann, U., Schwarz, J.P., Shindell,
257 D., Storelvmo, T., Warren, S.G., Zender, C.S., 2013. Bounding the role of black carbon in the
258 climate system: A scientific assessment. *J. Geophys. Res.* 118, 5380-5552.
- 259 Cappa, C.D., Onasch, T.B., Massoli, P., Worsnop, D.R., Bates, T.S., Cross, E.S., Davidovits, P.,
260 Hakala, J., Hayden, K.L., Jobson, B.T., Kolesar, K.R., Lack, D.A., Lerner, B.M., Li, S.-M.,
261 Mellon, D., Nuaaman, I., Olfert, J.S., Petäjä, T., Quinn, P.K., Song, C., Subramanian, R.,
262 Williams, E.J., Zaveri, R.A., 2012. Radiative Absorption Enhancements Due to the Mixing State
263 of Atmospheric Black Carbon. *Science* 337, 1078-1081.
- 264 Cappa, C.D., Zhang, X., Russell, L.M., Collier, S., Lee, A.K.Y., Chen, C.-L., Betha, R., Chen, S., Liu,
265 J., Price, D.J., Sanchez, K.J., McMeeking, G.R., Williams, L.R., Onasch, T.B., Worsnop, D.R.,
266 Abbatt, J., Zhang, Q., 2019. Light absorption by ambient black and brown carbon and its
267 dependence on black carbon coating state for two California, USA cities in winter and summer.
268 *Journal of Geophysical Research: Atmospheres*.
- 269 Chandra, S., 2004. Can the state of mixing of black carbon aerosols explain the mystery of 'excess'
270 atmospheric absorption? *Geophysical Research Letters* 31.
- 271 Chung, S.H., Seinfeld, J.H., 2008. Climate response of direct radiative forcing of anthropogenic
272 black carbon. *Journal of Geophysical Research Atmospheres* 110, -.
- 273 Cui, X., Wang, X., Yang, L., Chen, B., Chen, J., Andersson, A., Gustafsson, O., 2016. Radiative
274 absorption enhancement from coatings on black carbon aerosols. *Sci Total Environ* 551-552,
275 51-56.
- 276 Flanner, M.G., Zender, C.S., Randerson, J.T., Rasch, P.J., 2007. Present-day climate forcing and
277 response from black carbon in snow. *Journal of Geophysical Research* 112.

278 Glen, C.C., 2010. Observations of secondary organic aerosol production and soot aging under
 279 atmospheric conditions using a novel environmental aerosol chamber. Dissertations & Theses -
 280 Gradworks.

281 Han, T., Xu, W., Chen, C., Liu, X., Wang, Q., Li, J., Zhao, X., Du, W., Wang, Z., Sun, Y., 2015.
 282 Chemical apportionment of aerosol optical properties during the Asia-Pacific Economic
 283 Cooperation summit in Beijing, China. *J. Geophys. Res.* 120, 12,281-212,295.

284 He, C., Liou, K.N., Takano, Y., Zhang, R., Levy Zamora, M., Yang, P., Li, Q., Leung, L.R., 2015.
 285 Variation of the radiative properties during black carbon aging: theoretical and experimental
 286 intercomparison. *Atmospheric Chemistry and Physics* 15, 11967-11980.

287 Hu, W., Hu, M., Hu, W., Jimenez, J.L., Yuan, B., Chen, W., Wang, M., Wu, Y., Chen, C., Wang, Z.,
 288 Peng, J., Zeng, L., Shao, M., 2016. Chemical composition, sources, and aging process of
 289 submicron aerosols in Beijing: Contrast between summer and winter. *Journal of Geophysical*
 290 *Research: Atmospheres* 121, 1955-1977.

291 Lack, D.A., Cappa, C.D., 2010. Impact of brown and clear carbon on light absorption enhancement,
 292 single scatter albedo and absorption wavelength dependence of black carbon. *Atmospheric*
 293 *Chemistry and Physics* 10, 4207-4220.

294 Lan, Z.-J., Huang, X.-F., Yu, K.-Y., Sun, T.-L., Zeng, L.-W., Hu, M., 2013. Light absorption of black
 295 carbon aerosol and its enhancement by mixing state in an urban atmosphere in South China.
 296 *Atmospheric Environment* 69, 118-123.

297 Lee, A.K.Y., Chen, C.-L., Liu, J., Price, D.J., Betha, R., Russell, L.M., Zhang, X., Cappa, C.D., 2017.
 298 Formation of secondary organic aerosol coating on black carbon particles near vehicular
 299 emissions. *Atmospheric Chemistry and Physics* 17, 15055-15067.

300 Liu, D., Joshi, R., Wang, J., Yu, C., Allan, J.D., Coe, H., Flynn, M.J., Xie, C., Lee, J., Squires, F.,
 301 Kotthaus, S., Grimmond, S., Ge, X., Sun, Y., Fu, P., 2018. Contrasting physical properties of
 302 black carbon in urban Beijing between winter and summer. *Atmos. Chem. Phys. Discuss.* 2018,
 303 1-30.

304 Liu, D., Whitehead, J., Alfarra, M.R., Reyes-Villegas, E., Spracklen, Dominick V., Reddington,
 305 Carly L., Kong, S., Williams, Paul I., Ting, Y.-C., Haslett, S., Taylor, Jonathan W., Flynn,

306 Michael J., Morgan, William T., McFiggans, G., Coe, H., Allan, James D., 2017. Black-carbon
307 absorption enhancement in the atmosphere determined by particle mixing state. *Nat. Geosci.* 10,
308 184-188.

309 Liu, S., Aiken, A.C., Gorkowski, K., Dubey, M.K., Cappa, C.D., Williams, L.R., Herndon, S.C.,
310 Massoli, P., Fortner, E.C., Chhabra, P.S., Brooks, W.A., Onasch, T.B., Jayne, J.T., Worsnop,
311 D.R., China, S., Sharma, N., Mazzoleni, C., Xu, L., Ng, N.L., Liu, D., Allan, J.D., Lee, J.D.,
312 Fleming, Z.L., Mohr, C., Zotter, P., Szidat, S., Prevot, A.S., 2015. Enhanced light absorption by
313 mixed source black and brown carbon particles in UK winter. *Nat. Commun.* 6, 8435.

314 Moteki, N., Kondo, Y., Miyazaki, Y., Takegawa, N., Komazaki, Y., Kurata, G., Shirai, T., Blake, D.R.,
315 Miyakawa, T., Koike, M., 2007. Evolution of mixing state of black carbon particles: Aircraft
316 measurements over the western Pacific in March 2004. *Geophysical Research Letters* 34.

317 Nakayama, T., Ikeda, Y., Sawada, Y., Setoguchi, Y., Ogawa, S., Kawana, K., Mochida, M., Ikemori,
318 F., Matsumoto, K., Matsumi, Y., 2015. Properties of light - absorbing aerosols in the Nagoya
319 urban area, Japan, in August 2011 and January 2012: Contributions of brown carbon and lensing
320 effect. *Journal of Geophysical Research Atmospheres* 119, 12,721-712,739.

321 Peng, J., Hu, M., Guo, S., Du, Z., Zheng, J., Shang, D., Levy, Z.M., Zeng, L., Shao, M., Wu, Y.S.,
322 2016. Markedly enhanced absorption and direct radiative forcing of black carbon under polluted
323 urban environments. *Proc. Natl. Acad. Sci. U.S.A.*

324 Shiraiwa, M., Kondo, Y., Iwamoto, T., Kita, K., 2010. Amplification of Light Absorption of Black
325 Carbon by Organic Coating. *Aerosol Science and Technology* 44, 46-54.

326 Stocker, T.F., Qin, D., Plattner, G.K., Tignor, M., Allen, S.K., Boschung, J., Nauels, A., Xia, Y., Bex,
327 V., Midgley, P.M., 2013. *Climate Change 2013: The Physical Science Basis*. Intergovernmental
328 Panel on Climate Change, Working Group I Contribution to the IPCC Fifth Assessment Report
329 (AR5). Cambridge University Press: New York.

330 Sun, J., Liu, L., Xu, L., Wang, Y., Wu, Z., Hu, M., Shi, Z., Li, Y., Zhang, X., Chen, J., Li, W., 2018.
331 Key Role of Nitrate in Phase Transitions of Urban Particles: Implications of Important Reactive
332 Surfaces for Secondary Aerosol Formation. *Journal of Geophysical Research: Atmospheres* 123,
333 1234-1243.

334 Sun, Y., Wang, Z., Dong, H., Yang, T., Li, J., Pan, X., Chen, P., Jayne, J.T., 2012. Characterization of
335 summer organic and inorganic aerosols in Beijing, China with an Aerosol Chemical Speciation
336 Monitor. *Atmospheric Environment* 51, 250-259.

337 Thamban, N.M., Tripathi, S.N., Moosakutty, S.P., Kuntamukkala, P., Kanawade, V.P., 2017.
338 Internally mixed black carbon in the Indo-Gangetic Plain and its effect on absorption
339 enhancement. *Atmospheric Research* 197, 211-223.

340 Ting, Y., Mitchell, E., Allan, J., Liu, D., Spracklen, D., Williams, A., Jones, J.M., Lea-Langton, A.R.,
341 McFiggans, G., Coe, H., 2018. The Mixing State of Carbonaceous Aerosols of Primary
342 Emissions from 'Improved' African Cookstoves. *Environ. Sci. Technol.*

343 Wang, J., Liu, D., Ge, X., Wu, Y., Shen, F., Chen, M., Zhao, J., Xie, C., Wang, Q., Xu, W., Zhang, J.,
344 Hu, J., Allan, J., Joshi, R., Fu, P., Coe, H., Sun, Y., 2019a. Characterization of black
345 carbon-containing fine particles in Beijing during wintertime. *Atmospheric Chemistry and
346 Physics* 19, 447-458.

347 Wang, J., X., G., Wu, Y., Shen, F., Chen, M., Zhao, J., Xie, C., Wang, Q., Xu, W., Sun, Y., 2019b.
348 Characterization of black carbon-containing fine particles in Beijing during summertime:
349 Contrast between SP-AMS and HR-AMS, in preparation.

350 Wang, Q., Huang, R.J., Cao, J., Han, Y., Wang, G., Li, G., Wang, Y., Dai, W., Zhang, R., Zhou, Y.,
351 2014a. Mixing State of Black Carbon Aerosol in a Heavily Polluted Urban Area of China:
352 Implications for Light Absorption Enhancement. *Aerosol Science and Technology* 48, 689-697.

353 Wang, Q., Jacob, D.J., Spackman, J.R., Perring, A.E., Schwarz, J.P., Moteki, N., Marais, E.A., Ge, C.,
354 Wang, J., Barrett, S.R.H., 2014b. Global budget and radiative forcing of black carbon aerosol:
355 Constraints from pole to pole (HIPPO) observations across the Pacific. *Journal of Geophysical
356 Research Atmospheres* 119, 195-206.

357 Wu, Y., Cheng, T., Liu, d., Allan, J., Zheng, L., Chen, H., 2018. Light absorption enhancement of
358 black carbon aerosol constrained by particle morphology. *Environmental Science &
359 Technology*.

360 Xie, C., Xu, W., Wang, J., Wang, Q., Liu, D., Tang, G., Chen, P., Du, W., Zhao, J., Zhang, Y., Zhou,
361 W., Han, T., Bian, Q., Li, J., Fu, P., Wang, Z., Ge, X., Allan, J., Coe, H., Sun, Y., 2019. Vertical

362 characterization of aerosol optical properties and brown carbon in winter in urban Beijing,
363 China. *Atmospheric Chemistry and Physics* 19, 165-179.

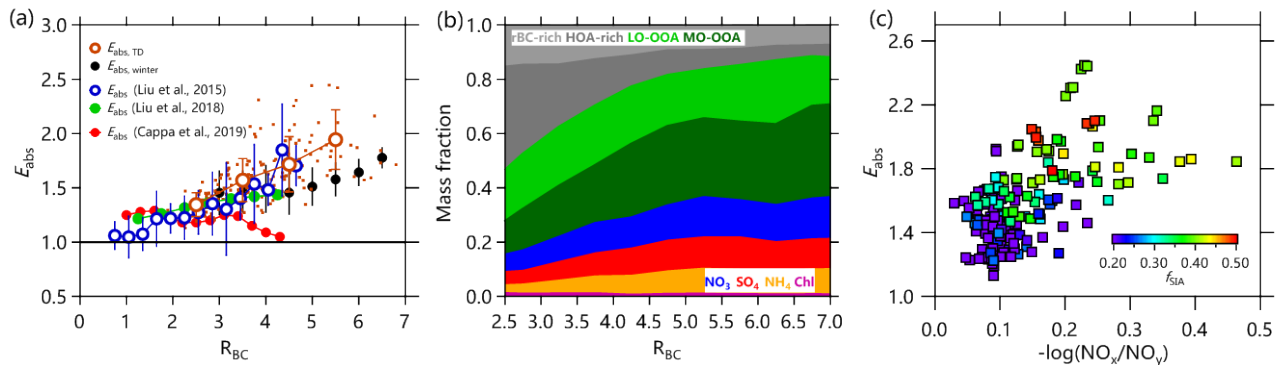
364 Xu, W., Xie, C., Karnezi, E., Zhang, Q., Wang, J., Pandis, S.N., Ge, X., Wang, Q., Zhao, J., Du, W.,
365 Qiu, Y., Zhou, W., He, Y., Zhang, J., An, J., Li, Y., Li, J., Fu, P., Wang, Z., Worsnop, D.R., Sun,
366 Y., 2019. Summertime aerosol volatility measurements in Beijing, China. *Atmospheric*
367 *Chemistry and Physics Discussions*, 1-19.

368 Zhang, Y., Favez, O., Canonaco, F., Liu, D., Močnik, G., Amodeo, T., Sciare, J., Prévôt, A.S.H., Gros,
369 V., Albinet, A., 2018a. Evidence of major secondary organic aerosol contribution to lensing
370 effect black carbon absorption enhancement. *npj Climate and Atmospheric Science* 1.

371 Zhang, Y., Zhang, Q., Cheng, Y., Su, H., Li, H., Li, M., Zhang, X., Ding, A., He, K., 2018b.
372 Amplification of light absorption of black carbon associated with air pollution. *Atmospheric*
373 *Chemistry and Physics* 18, 9879-9896.

374 Zhao, J., Du, W., Zhang, Y., Wang, Q., Chen, C., Xu, W., Han, T., Wang, Y., Fu, P., Wang, Z., Li, Z.,
375 Sun, Y., 2017. Insights into aerosol chemistry during the 2015 China Victory Day parade: results
376 from simultaneous measurements at ground level and 260 m in Beijing. *Atmos. Chem. Phys.* 17,
377 3215-3232.

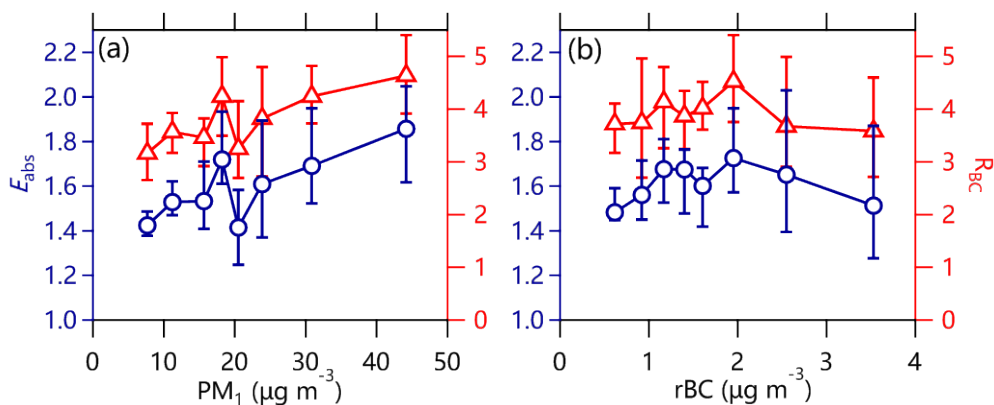
378



379

380 Fig. 1. (a) BC absorption enhancement as a function of R_{BC} . Also shown are the E_{abs} measurements
 381 at 532 nm in UK winter (Liu et al., 2015) and Fresno, California (Cappa et al., 2019). The E_{abs} in
 382 winter in Beijing was calculated as the MAC divided by $7.4 \text{ m}^2 \text{ g}^{-1}$ (Xie et al., 2019). In addition, E_{abs}
 383 in Beijing summer was also modeled with the SP2 measurements (Liu et al., 2018). The error bars in
 384 the figure are one standard deviations. (b) Chemical composition of rBC coatings as a function of
 385 R_{BC} , and (c) scatter plot of E_{abs} versus $-\log(\text{NO}_x/\text{NO}_y)$ color coded by the fraction of secondary
 386 inorganic aerosol (f_{SIA}).

387

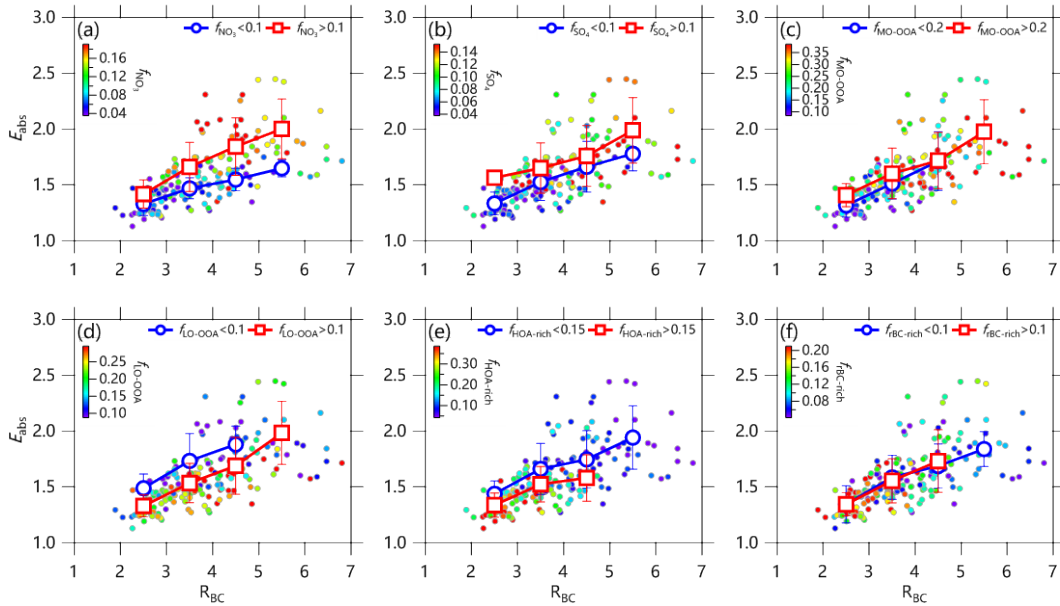


388

389

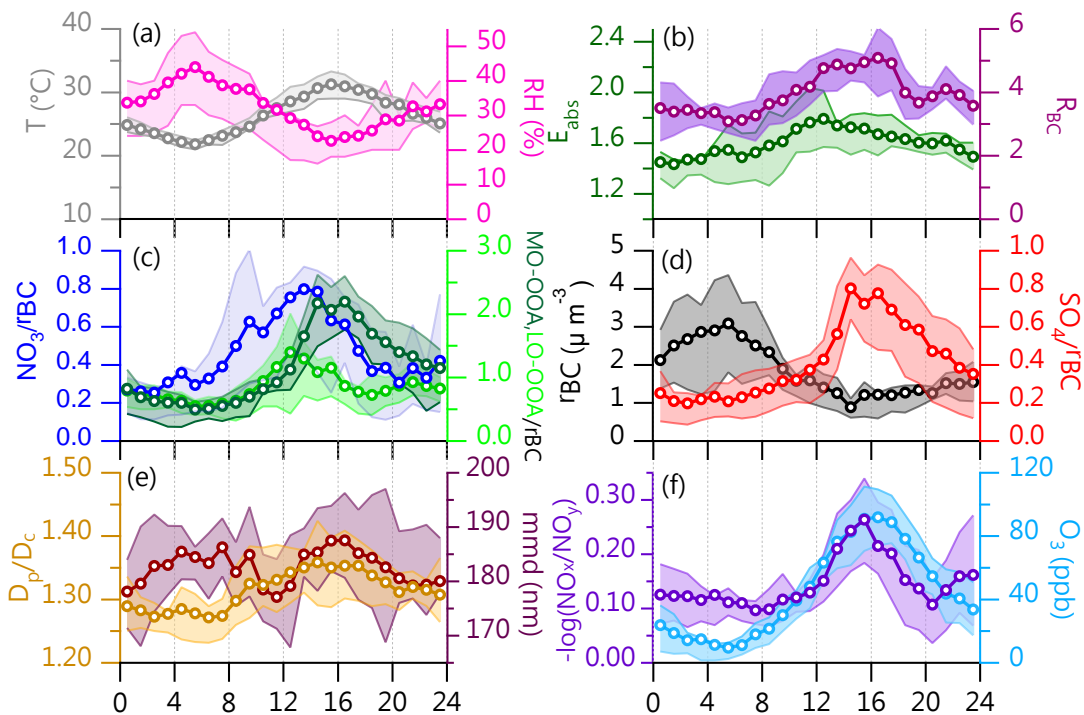
390 Fig. 2. Variations of E_{abs} and R_{BC} as a function of (a) PM_1 mass loadings and (b) rBC concentrations.
 391 The bottom and top error bars represent 25th and 75th percentiles.

392



393

394 Fig. 3. Variations of BC absorption enhancement as a function of R_{BC} , color coded by mass fractions
 395 of (a) NO_3 , (b) SO_4 , (c) MO-OOA, (d) LO-OOA, (e) HOA-rich, (f) rBC-rich in rBC coatings.
 396 The data were binned with low (red squares) and high (blue circles) mass fraction of each aerosol species,
 397 and the error bars are one standard deviations.



398

399 Fig. 4. Diurnal variations of (a) temperature (T) and relative humidity (RH), (b) E_{abs} and R_{BC} , (c)
 400 mass ratios of NO_3 , MO-OOA, and LO-OOA to rBC, (d) rBC and mass ratio of SO_4 to rBC, (e)
 401 D_p/D_c and mass median diameter of rBC, and (f) $-\log(\text{NO}_x/\text{NO}_y)$ and O_3 . The circles are mean values,
 402 and the shaded areas represent 25th and 75th percentiles.